Delta-X: AVIRIS-NG BRDF-Adjusted Surface Reflectance and Mosaics, MRD, LA, 2021, V3

Get Data

Documentation Revision Date: 2025-02-06

Dataset Version: 3

Summary

This data provides AVIRIS-NG Bidirectional Reflectance Distribution Function (BRDF) and sunglint-corrected surface spectral reflectance images over the Atchafalaya and Terrebonne basins of the Mississippi River Delta (MRD) of coastal Louisiana, USA. Flights were acquired during the Spring and Fall 2021 deployments of the Delta-X campaign. The imagery was acquired by the Airborne Visible/Infrared Imaging Spectrometer - Next Generation (AVIRIS-NG) from 2021-03-27 to 2021-04-06 and 2021-08-18 to 2021-09-25. Reflectance data are provided for each flight line. In addition, ten files of mosaicked flight lines, by time period and over four locations (labeled Terre, Atcha, TerreEast, and Bara), are included. Data are provided as binary ENVI image and header files. Only land pixels were corrected; mask files for the mosaic file coverage showing presence/absence of water and clouds are also included. For the Delta-X mission, these data serve to better understand rates of soil erosion, accretion, and creation in the delta system, with the goal of building better models of how river deltas will behave under relative sea level rise.

In this Version 3, the 10 mosaic files and the 10 associated mask files have been updated. Please see Section 8: Dataset Revisions for additional details.

This dataset contains a total of 440 files. There are 220 ENVI images. Each ENVI includes two files: a multiband binary (*.dat) and a corresponding header (*.hdr) file containing metadata.

Figure 1: A BRDF and sunglint-corrected image of the Atchafalaya basin in coastal Louisiana, U.S.

Citation

Thompson, D.R., D.J. Jensen, J.W. Chapman, M. Simard, and E. Greenberg. 2025. Delta-X: AVIRIS-NG BRDF-Adjusted Surface Reflectance and Mosaics, MRD, LA, 2021, V3. ORNL DAAC, Oak Ridge, Tennessee, USA. https://doi.org/10.3334/ORNLDAAC/2355

Table of Contents

1. Dataset Overview
2. Data Characteristics
3. Application and Derivation
4. Quality Assessment
5. Data Acquisition, Materials, and Methods
6. Data Access
7. References
8. Dataset Revisions

1. Dataset Overview

This data provides AVIRIS-NG Bidirectional Reflectance Distribution Function (BRDF) and sunglint-corrected surface spectral reflectance images over the Atchafalaya and Terrebonne basins of the Mississippi River Delta (MRD) of coastal Louisiana, USA. Flights were acquired during the Spring and Fall 2021 deployments of the Delta-X campaign. The imagery was acquired by the Airborne Visible/Infrared Imaging Spectrometer - Next Generation (AVIRIS-NG) from 2021-03-27 to 2021-04-06 and 2021-08-18 to 2021-09-25. Reflectance data are provided for each flight line. In addition, ten files of mosaicked flight lines, by time period and over four locations (labeled Terre, Atcha, TerreEast, and Bara), are included. Data are provided as binary ENVI image and header files. Only land pixels were corrected; mask files for the mosaic file coverage showing presence/absence of water and clouds are also included. For the Delta-X mission, these data serve to better understand rates of soil erosion, accretion, and creation in the delta system, with the goal of building better models of how river deltas will behave under relative sea level rise.

Project: Delta-X

The Delta-X mission is a 5-year NASA Earth Venture Suborbital-3 mission to study the Mississippi River Delta in the United States, which is growing and sinking in different areas. River deltas and their wetlands are drowning as a result of sea level rise and reduced sediment inputs. The Delta-X mission will determine which parts will survive and continue to grow, and which parts will be lost. Delta-X begins with airborne and in situ data acquisition and carries through data analysis, model integration, and validation to predict the extent and spatial patterns of future deltaic land loss or gain.

Related Datasets:

Thompson, D.R., D.J. Jensen, J.W. Chapman, M. Simard, and E. Greenberg. 2023. Delta-X: AVIRIS-NG L2B BRDF-Adjusted Surface Reflectance, MRD, LA, 2021, V2. ORNL DAAC, Oak Ridge, Tennessee, USA. https://doi.org/10.3334/ORNLDAAC/2139

- Version 2 of this dataset

Thompson, D.R., D.J. Jensen, J.W. Chapman, M. Simard, and E. Greenberg. 2022. Delta-X: AVIRIS-NG BRDF-Adjusted Surface Reflectance, MRD, LA, 2021. ORNL DAAC, Oak Ridge, Tennessee, USA. https://doi.org/10.3334/ORNLDAAC/2025

- Version 1 of this dataset. Now superseded.

Thompson, D.R., D.J. Jensen, J. Chapman, E. Greenberg, and M. Simard. 2022. Delta-X: AVIRIS-NG L1B Spectral Radiance Products, MRD, Louisiana, 2021. ORNL DAAC, Oak Ridge, Tennessee, USA. https://doi.org/10.3334/ORNLDAAC/1987

- Outputs from an earlier processing step in the the production of the Delta-X surface reflectance products

Thompson, D.R., D.J. Jensen, J. Chapman, E. Greenberg, and M. Simard. 2022. Delta-X AVIRIS-NG L2 Surface Reflectance Products across the MRD, LA, USA, 2021. ORNL DAAC, Oak Ridge, Tennessee, USA. https://doi.org/10.3334/ORNLDAAC/1988.

- Outputs from an earlier processing step in the the production of the Delta-X surface reflectance products

Fichot, C.G., and J. Harringmeyer. 2022. Delta-X: Spectral Reflectance of Water Surface Across MRD, LA, USA, Spring 2021. ORNL DAAC, Oak Ridge, Tennessee, USA. https://doi.org/10.3334/ORNLDAAC/1994.

- In situ reflectance measurements used for calibration and validation of Delta-X AVIRIS-NG surface reflectance products

Jensen, D.J., D.R. Thompson, I.B. Mccubbin, and M. Simard. 2021. Pre-Delta-X: L2 AVIRIS-NG Surface Spectral Reflectance across MRD, LA, USA, 2015-2016. ORNL DAAC, Oak Ridge, Tennessee, USA. https://doi.org/10.3334/ORNLDAAC/1826

- L2 surface reflectance products from Pre-Delta-X

Acknowledgement

This research was funded by the NASA Earth Venture Suborbital (EVS-3) program, grant NNH17ZDA001N-EVS3.

2. Data Characteristics

Spatial Coverage: Atchafalaya and Terrebonne basins, Mississippi River Delta (MRD), Louisiana, USA

Spatial Resolution: Approximately 3.8 to 5.4 m

Temporal Coverage: 2021-03-27 to 2021-09-25

Temporal Resolution: Multiple overpasses at irregular intervals

Spectral Parameters: 425 bands at 5-nm resolution with a range between 380 - 2500 nm

Study Area: Latitude and longitude are given in decimal degrees.

Site	Westernmost Longitude	Easternmost Longitude	Northernmost Latitude	Southernmost Latitude
Atchafalaya and Terrebonne basins, Louisiana, US	-91.5892	-89.0721	30.2262	29.1797

Data File Information

This dataset contains a total of 440 files. There are 220 ENVI images. Each ENVI includes two files: a multiband binary (*.dat) and a corresponding header (*.hdr) file containing metadata in text format.

There are three types of ENVI files:

- *Corrected surface reflectance for single flight line*: 200 ENVIs of BRDF- and sunglint-corrected surface reflectance measurements for an individual flight line
- *Mosaics of flight lines*: 10 ENVIs of BRDF- and sunglint-corrected surface reflectance measurements as a mosaic of flight lines with fine-grained orthorectification within a region of the study area (Table 2)
- *Land mask files*: 10 data ENVIs providing presence (1) or absence (0) of land over the same extent as the mosaics of flight lines, along with cloud (2) and cloud shadow (3) presence.

File Naming Conventions

- Individual reflectance flight lines: **ang<*YYYYMMDD*t*hhmmss*>_rfl_brdf.<*ext*>**, where
  - <***YYYYMMDD*t*hhmmss***> = the date (*YYYYMMDD*) and time (*hhmmss*) of data acquisition in UTC
  - **rfl** = indicates reflectance
  - **brdf** = indicates Bidirectional Reflectance Distribution Function corrections
  - <***ext***> = file type: "dat" for ENVI binary and "hdr" for ENVI header file
- The header (.hdr) for each flight line ENVI holds metadata for the binary data file, including:
  - number of samples (cols), lines (rows), and bands
  - data type (4 = Float32, 5 = Float64, interleave type, and byte order
  - map info: projection and datum, coordinates for x y reference points, pixel size, and map units
  - no data value

The flight line ENVI files are in a rotated UTM projection that follows the trajectory of the respective flight path.

- Mosaics of reflectance flight lines: **ang<*YYYYMMDD*>_rfl_brdf_<*loc*>.<*ext*>**, where
  - ***YYYYMMDD*** = the date of data acquisition in UTC. Some files include multiple dates, these are formatted ***YYYYMMDD-DD***, where the first ***DD*** is the start date and the second ***DD*** is the end date)
  - <***loc***> is the location abbreviation: "Atcha", "Bara", "Terre", or "TerreEast"
- Land mask files **angYYYYMMDD_rfl_brdf_<*loc*>_mask.<*ext*>**, where
  - **mask** indicates an analysis masks where 0: land absent, 1: land present, 2: cloud present, and 3: cloud shadow present.

The reflectance files have:

- Bands at 5-nm resolution covering wavelengths from 380 - 2500 nm
- Horizontal spatial resolution is 3.8 - 5.4 m raster cells
- The range of valid surface reflectance values is 0.0 - 1.0
- No data values are indicated by -9999

Table 1. ENVI file metadata contained in the header (*.hdr) files.

Variable	Description
samples	number of columns in image file
lines	number of rows in the image file
data ignore value	no data value
wavelength units	units for band wavelengths
wavelength	a vector of wavelength values, one per band
fwhm	full width at half maximum, a vector of values, one for each band, measuring spectral resolution
smoothing factors	a vector of values, one for each band, used for reducing noise in reflectance values

Table 2. Mosaic File names and file sizes.

Mosaic File Name	Size (GB)
ang20210401_rfl_brdf_Atcha.dat	108
ang20210820-22_rfl_brdf_Atcha.dat	109
ang20210924_rfl_brdf_Atcha.dat	109
ang20210924-25_rfl_brdf_Bara.dat	61
ang20210402-05_rfl_brdf_Bara.dat	63
ang20210402-05_rfl_brdf_Terre.dat	232
ang20210823-25_rfl_brdf_Terre.dat	229

Mosaic File Name	Size (GB)
ang20210923_rfl_brdf_Terre.dat	229
ang20210402-04_rfl_brdf_TerreEast.dat	73
ang20210924-25_rfl_brdf_TerreEast.dat	73

3. Application and Derivation

Surface reflectance spectra are commonly used to measure properties of the surface composition. They can indicate water column constituents, soil composition, vegetation functional traits, and more. For a description of the imaging spectroscopy measurement and its applications to different Earth science disciplines (see Cawse-Nicholson et al., 2021).

4. Quality Assessment

Data quality was monitored at several steps during acquisition and analysis. First, operators performed a preliminary assessment using a real-time display in the cabin by monitoring images and spectra in a scrolling “waterfall” plot. This assessment allowed identification of impinging clouds, instrument artifacts, or other issues that would require adjustment or (in the worst case) immediate reacquisition. Second, representative spectra were used to assess the performance of science data algorithms at each stage. These could be matched to in-situ reference data in order to validate calibration as well as estimate uncertainty following procedures outlined in Thompson et. al. (2019a, 2019b). In general, the campaign data from spring 2021 have superior surface reflectance estimation due to the better atmospheric conditions encountered during those flights. Fall 2021 overflights encountered higher atmospheric haze and water vapor loadings, with a larger number of clouds.

Bad data flags (-9999, noted in header information) were embedded in the spectroscopic data. These flags serve mainly to mark the periphery of an orthorectified image where no spectra were acquired. Clouds and other valid but unusable regions were still considered bona fide scene content and not altered. However, for surface studies authors recommend ignoring a large margin of data (1 km or more) around any visible clouds to avoid their disruption to the downwelling incident light field and corresponding increase in atmospheric correction error.

5. Data Acquisition, Materials, and Methods

AVIRIS-NG is a pushbroom spectral mapping system with a high signal-to-noise ratio (SNR) designed for high performance spectroscopy. AVIRIS-NG was developed as a successor to the Classic Airborne Visible Infrared Imaging Spectrometer (AVIRIS-C) (Green et al., 1998). The instrument covers the entire solar reflected spectrum from 380-2510 nm with a single Focal Plane Array (FPA), at a spectral sampling of approximately 5 nm. The AVIRIS- NG sensor has a 1 milliradian instantaneous field of view, providing altitude-dependent ground sampling distance ranging from sub-meter to 20 m scales. Its detector has a 640×480-pixel array, from which standard products are generated using the sensor’s 600 cross-track spatial samples and 425 spectral samples. Each acquisition is a “flight line” forming a continuous strip of pushbroom data that typically takes 1-10 minutes to acquire. Multiple aircraft overflights cover the region of interest in these strips, accumulating a combined map of the target area. For this campaign, AVIRIS-NG was implemented on a Dynamic Aviation King Air B200. The instrument has four components: 1) a sensor with its mount and camera glass mounted at a nadir port; 2) an onboard calibrator (OBC), mounted in the cabin next to the sensor; 3) a forward operator electronics rack, and 4) an aft thermal-control electronics rack.

AVIRIS-NG acquired data in its standard operating mode over regions of interest in the Atchafalaya and Terrebonne basins. The area was provisionally split into multiple mosaics— a large “survey” covering the entire domain—which required multiple days to complete. Flight lines had a 15% overlap area at their margins to accommodate position and geometric sampling uncertainty. The precise direction of flight lines was adjusted to accommodate local time and weather conditions and to ameliorate sun glint effects. Because AVIRIS-NG’s data collection was impeded when clouds were present below or above the aircraft, the team typically decided which days to fly based on an early morning “go/no-go” decision from the daily weather forecast.

The AVIRIS-NG radiance data (Level 1B) were derived by calibrating incident radiance spectra measured by the sensor using the techniques described in Thompson et al. (2018a, 2018b) and Chapman et al. (2019). These radiances were then analyzed to estimate atmospheric state and surface reflectance (Level 2) using the method of Thompson et al. (2018a, 2018b, 2019a). During this stage, a vicarious radiometric correction on the order of 1% is applied which evens out minor discrepancies between the laboratory calibration and flight conditions. This vicarious adjustment uses an in situ reference from the Delta-X flight campaign, and a correction procedure detailed in Bruegge et al. (2021). The observed reflectance signal is influenced by the bi-directional reflectance distribution function (BRDF) resulting from variation in solar and instrument viewing angles, manifesting in differences in illumination intensity across various surface cover types within each scene. The BRDF effects were estimated and corrected using the algorithm described in Queally et al. (2022). Only land pixels were corrected in this way; water pixels, which were recognized by a band ratio combination (Greenberg et al., 2022), were instead adjusted to remove specular sunglint using the approach in Gao and Li (2021). This processing cascade is visualized in Figure 2.

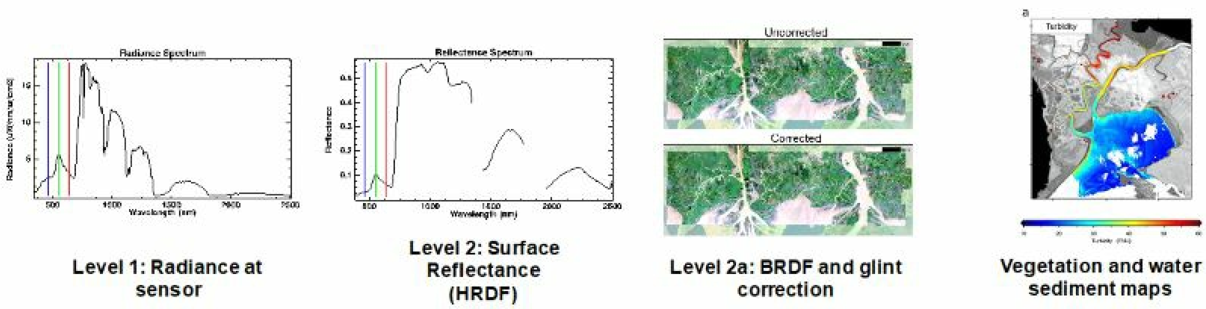

Figure 2: AVIRIS-NG data processing chain, showing the progression from Radiance (Level 1) products to Reflectance (Level 2), BRDF and sunglint correction (Level 2B); image from Greenberg et al., 2022, and Vegetation and water property maps (Level 3); image from Fichot et al., 2016.

Each mosaic of surface reflectance data was produced using the BRDF and sunglint-corrected flightlines, with an addition fine-grained orthorectification applied to each flightline. Following Wang et al. (2023), each flightline was processed through a “rubber sheet” correction algorithm in Google Earth Engine using Sentinel 2 reference images collected on April 20 and 22, 2021. This algorithm aligned the features along the edges of each flightline, reducing georectification errors along the mosaic seams. Masks of each of these rectified mosaic datasets were generated to divide land pixels from water, using a Normalized Difference Water Index threshold of 0.1. In addition, clouds and cloud shadows were classified, buffered, and added to the mask data.

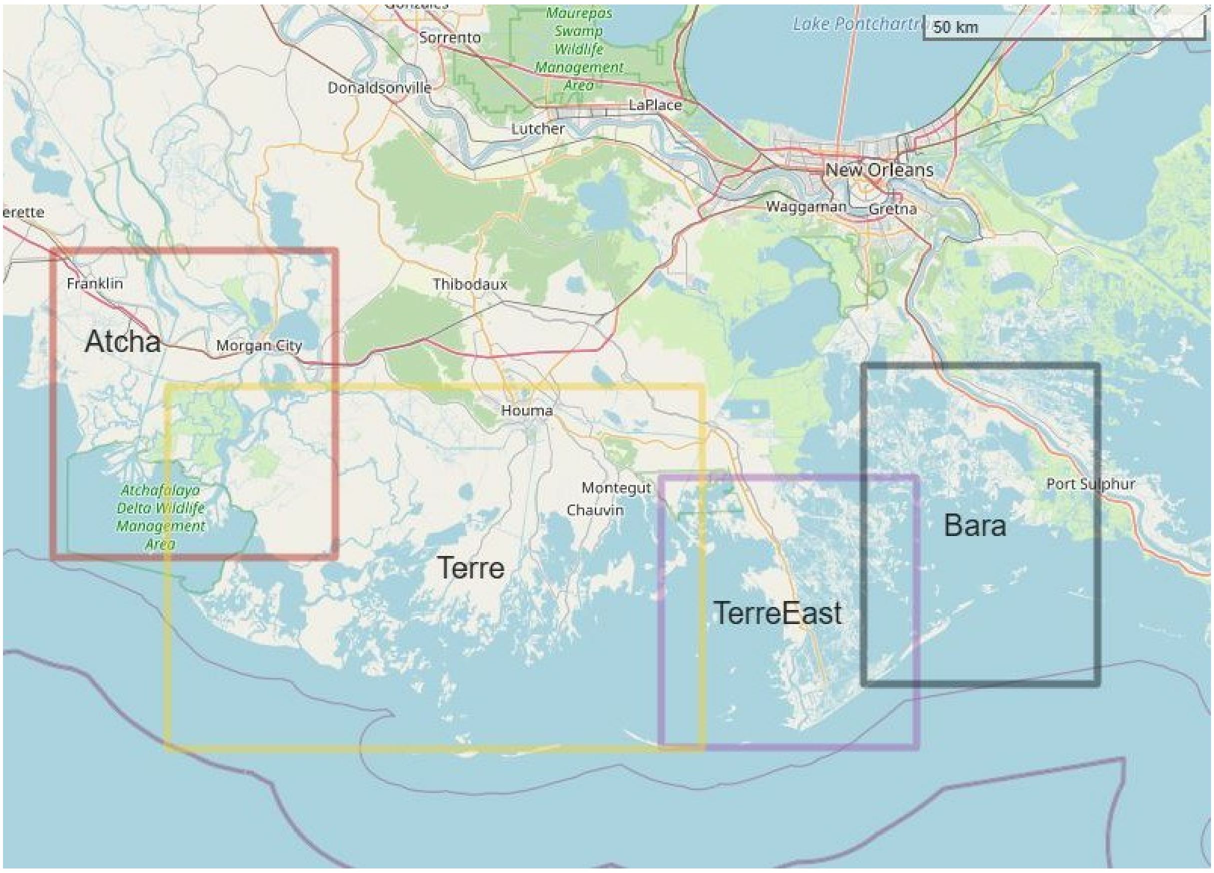

Figure 3. Approximate location of the flight line mosaics in coastal Louisiana, US, labeled by basins: "Atcha" = Atchafalaya, "Terre" = Terrebonne, "TerreEast" = eastern Terrebonne, "Bara" = Barataria. Basemap: © OpenStreetMap contributors.

6. Data Access

These data are available through the Oak Ridge National Laboratory (ORNL) Distributed Active Archive Center (DAAC).

Delta-X: AVIRIS-NG BRDF-Adjusted Surface Reflectance and Mosaics, MRD, LA, 2021, V3

Contact for Data Center Access Information:

- E-mail: uso@daac.ornl.gov
- Telephone: +1 (865) 241-3952

7. References

Bruegge, C.J., G.T. Arnold, J. Czapla-Myers, R. Dominguez, M.C. Helmlinger, D.R. Thompson, J.V. den Bosch, and B.N. Wenny. 2021. Vicarious Calibration of eMAS, AirMSPI, and AVIRIS Sensors During FIREX-AQ. IEEE Transactions on Geoscience and Remote Sensing 59:10286–10297. https://doi.org/10.1109/TGRS.2021.3066997.

Cawse-Nicholson, K., P.A. Townsend, D. Schimel, A.M. Assiri, P.L. Blake, M.F. Buongiorno, P. Campbell, N. Carmon, K.A. Casey, R.E. Correa-Pabón, K.M. Dahlin, H. Dashti, P.E. Dennison, H. Dierssen, A. Erickson, J.B. Fisher, R. Frouin, C.K. Gatebe, H. Gholizadeh, M. Gierach, N.F. Glenn, J.A. Goodman, D.M. Griffith, L. Guild, C.R. Hakkenberg, E.J. Hochberg, T.R. H. Holmes, C. Hu, G. Hulley, K.F. Huemmrich, R.M. Kudela, R.F. Kokaly, C.M. Lee, R. Martin, C.E. Miller, W.J. Moses, F.E. Muller-Karger, J.D. Ortiz, D.B. Otis, N. Pahlevan, T.H. Painter, R. Pavlick, B. Poulter, Y. Qi, V.J. Realmuto, D. Roberts, M.E. Schaepman, F.D. Schneider, F.M. Schwandner, S.P. Serbin, A.N. Shiklomanov, E.N. Stavros, D.R. Thompson, J.L. Torres-Perez, K.R. Turpie, M. Tzortziou, S. Ustin, Q. Yu, Y. Yusup, and Q. Zhang. 2021. NASA's surface biology and geology designated observable: A perspective on surface imaging algorithms. Remote Sensing of Environment 257:112349. https://doi.org/10.1016/j.rse.2021.112349.

Chapman, J.W., D.R. Thompson, M.C. Helmlinger, B.D. Bue, R.O. Green, M.L. Eastwood, S. Geier, W. Olson-Duvall, and S.R. Lundeen. 2019. Spectral and radiometric calibration of the Next Generation Airborne Visible Infrared Spectrometer (AVIRIS-NG). Remote Sensing 11:2129. https://doi.org/10.3390/rs11182129.

Fichot, C.G., and J. Harringmeyer. 2022. Delta-X: Spectral Reflectance of Water Surface Across MRD, LA, USA, Spring 2021. ORNL DAAC, Oak Ridge, Tennessee, USA. https://doi.org/10.3334/ORNLDAAC/1994.

Fichot, C.G., B.D. Downing, B.A. Bergamaschi, L. Windham-Myers, M. Marvin-DiPasquale, D.R. Thompson, and M.M. Gierach. 2016. High-resolution remote sensing of water quality in the San Francisco Bay–Delta Estuary. Environmental Science & Technology 50:573–583. https://doi.org/10.1021/acs.est.5b03518.

Gao, B.C., and R.-R. Li. 2021. Correction of sunglint effects in high spatial resolution hyperspectral imagery using SWIR or NIR bands and taking account of spectral variation of refractive index of water: Advances in Environmental and Engineering Research 2:16.

https://doi.org/10.21926/aeer.2103017.

Green, R.O., M.L. Eastwood, C.M. Sarture, T.G. Chrien, M. Aronsson, B.J. Chippendale, J.A. Faust, B.E. Pavri, C.J. Chovit, M. Solis, M.R. Olah, and O. Williams. 1998. Imaging spectroscopy and the Airborne Visible/Infrared Imaging Spectrometer (AVIRIS). Remote Sensing of Environment 65:227–248. https://doi.org/10.1016/S0034-4257(98)00064-9.

Greenberg, E., D.R. Thompson, D. Jensen, P.A. Townsend, N. Queally, A. Chlus, C.G. Fichot, J.P. Harringmeyer, and M. Simard. 2022. An improved scheme for correcting remote spectral surface reflectance simultaneously for terrestrial BRDF and water-surface sunglint in coastal environments. Journal of Geophysical Research: Biogeosciences 127:e2021JG006712. https://doi.org/10.1029/2021JG006712

Jensen, D.J., D.R. Thompson, I.B. Mccubbin, and M. Simard. 2021. Pre-Delta-X: L2 AVIRIS-NG Surface Spectral Reflectance across MRD, LA, USA, 2015-2016. ORNL DAAC, Oak Ridge, Tennessee, USA. https://doi.org/10.3334/ORNLDAAC/1826

Queally, N., Z. Ye, T. Zheng, A. Chlus, F. Schneider, R. Pavlick, and P. A. Townsend. 2022. FlexBRDF: A flexible BRDF correction for grouped processing of airborne imaging spectroscopy flightlines. Journal of Geophysical Research: Biogeosciences 127:e2021JG006622. https://doi.org/10.1029/2021JG006622.

Thompson, D.R., D.J. Jensen, J. Chapman, E. Greenberg, and M. Simard. 2022. Delta-X: AVIRIS-NG L1B Spectral Radiance Products, MRD, Louisiana, 2021. ORNL DAAC, Oak Ridge, Tennessee, USA. https://doi.org/10.3334/ORNLDAAC/1987

Thompson, D.R., D.J. Jensen, J. Chapman, E. Greenberg, and M. Simard. 2022. Delta-X AVIRIS-NG L2 Surface Reflectance Products across the MRD, LA, USA, 2021. ORNL DAAC, Oak Ridge, Tennessee, USA. https://doi.org/10.3334/ORNLDAAC/1988.

Thompson, D.R., D.J. Jensen, J.W. Chapman, M. Simard, and E. Greenberg. 2022. Delta-X: AVIRIS-NG BRDF-Adjusted Surface Reflectance, MRD, LA, 2021. ORNL DAAC, Oak Ridge, Tennessee, USA. https://doi.org/10.3334/ORNLDAAC/2025

Thompson, D.R., D.J. Jensen, J.W. Chapman, M. Simard, and E. Greenberg. 2023. Delta-X: AVIRIS-NG L2B BRDF-Adjusted Surface Reflectance, MRD, LA, 2021, V2. ORNL DAAC, Oak Ridge, Tennessee, USA. https://doi.org/10.3334/ORNLDAAC/2139

Thompson, D.R., K. Cawse-Nicholson, Z. Erickson, C.G. Fichot, C. Frankenberg, B.-C. Gao, M.M. Gierach, R.O. Green, D. Jensen, V. Natraj, and A. Thompson. 2019a. A unified approach to estimate land and water reflectances with uncertainties for coastal imaging spectroscopy. Remote Sensing of Environment 231:111198. https://doi.org/10.1016/j.rse.2019.05.017.

Thompson, D.R., L. Guanter, A. Berk, B.-C. Gao, R. Richter, D. Schläpfer, and K.J. Thome. 2019b. Retrieval of atmospheric parameters and surface reflectance from visible and shortwave infrared imaging spectroscopy data. Surveys in Geophysics 40:333–360. https://doi.org/10.1007/s10712-018-9488-9.

Thompson, D.R., J.W. Boardman, M.L. Eastwood, R.O. Green, J.M. Haag, P. Mouroulis, and B. Van Gorp. 2018a. Imaging spectrometer stray spectral response: In-flight characterization, correction, and validation. Remote Sensing of Environment 204:850–860. https://doi.org/10.1016/j.rse.2017.09.015.

Thompson, D.R., V. Natraj, R.O. Green, M.C. Helmlinger, B.-C. Gao, and M.L. Eastwood. 2018b. Optimal estimation for imaging spectrometer atmospheric correction. Remote Sensing of Environment 216:355–373. https://doi.org/10.1016/j.rse.2018.07.003.

Wang, C., T.M. Pavelsky, E.D. Kyzivat, F. Garcia-Tigreros, E. Podest, F. Yao, X. Yang, S. Zhang, C. Song, T. Langhorst, W. Dolan, M.R. Kurek, M.E. Harlan, L.C. Smith, D.E. Butman, R.G.M. Spencer, C.J. Gleason, K.P. Wickland, R.G. Striegl, and D.L. Peters. 2023. Quantification of wetland vegetation communities features with airborne AVIRIS-NG, UAVSAR, and UAV LiDAR data in Peace-Athabasca Delta. Remote Sensing of Environment 294:113646. https://doi.org/10.1016/j.rse.2023.113646

8. Dataset Revisions

Version	Release Date	Description
3	2025-02-06	The 10 mosaic files and 10 associated mask files were updated as follows: • Performed a fine-grained ortho-rectification on all flightlines in each mosaic and mask file to correct offset alignment along image borders. • Added buffered cloud and shadow classes to all mask files. • Removed dark pixels at the end of flightlines caused by the AVIRIS-NG instrument shutter No other files have been altered.
2	2023-06-07	Five compressed (*.zip) files were updated: • ang20210402-05_rfl_brdf_Terre (Updated to include missing flightline) • ang20210402-05_rfl_brdf_Terre_mask (Updated to include a cloud shadow class and additional corrections performed to land/water extents) • ang20210820-22_rfl_brdf_Atcha_mask (Updated to include a cloud shadow class) • ang20210823-25_rfl_brdf_Terre_mask (Updated to include a cloud shadow class) • ang20210924_rfl_brdf_Atcha (Updated version corrects a band that was corrupted) No other files have been altered.
1	2022-08-31	Original publication